

The Seismotectonics and Seismicity of the Laptev Sea Region: The Current Situation and a First Experience in a Year-Long Installation of Ocean Bottom Seismometers on the Shelf

A. A. Krylov^{a, b, *}, A. I. Ivashchenko^a, S. A. Kovachev^a, N. V. Tsukanov^a, M. E. Kulikov^a,
I. P. Medvedev^a, D. A. Ilinskiy^{a, b}, and N. E. Shakhova^{c, d}

^a*Shirshov Institute of Oceanology (IO), Russian Academy of Sciences (RAS), Nakhimovsky prosp., 36, Moscow, 117997 Russia*

^b*Moscow Institute of Physics and Technology (MIPT), Institutsky per., 9, Dolgoprudnyi, Moscow Region., 141701 Russia*

^c*Tomsk National State Research University, Lenina prosp., 36, Tomsk, 634050 Russia*

^d*International Arctic Research Center, University of Alaska Fairbanks,
Koyukuk Dr. str., 2160, PO Box 757340, Fairbanks, AK 99775 USA*

**e-mail: artyomkrlyv@ocean.ru*

Received July 4, 2020; revised August 7, 2020; accepted August 20, 2020

Abstract—This paper is a review of current concepts concerning the seismotectonics and seismicity in the Laptev Sea region. The chief feature of the region is a rift system extending in the shelf from the continental slope with the adjacent Gakkel Ridge to the mainland coast. There are several models to describe the present-day evolution of the region, but no one of these is preferable because of the lack of local instrumental observations of shelf microseismicity, while such microseismicity is characteristic of rift zones. One alternative approach consists in the installation of ocean bottom seismometers on the shelf itself. During the 73rd cruise of the R/V *Akademik Mstislav Keldysh*, a temporary network was deployed consisting of 7 broadband bottom seismic stations on the Laptev Sea shelf. Comparative analysis of noise spectra based on records of a hydrophone, a bottom seismograph, and a wavegauge, showed that the noise amplitude strongly depends on wind waves, which is in turn dependent on marine ice cover, so that the recording potential of a local network of bottom seismographs is restricted to the winter period of observation.

Keywords: seismotectonics, seismicity, shelf, Laptev Sea, temporary local observing networks, ocean bottom seismometers

DOI: 10.1134/S0742046320060044

INTRODUCTION

The shelf of the Laptev Sea is one of the key regions of the Earth where a mid-oceanic spreading ridge (Gakkel Ridge) is adjacent to a continental rift zone. The goal of the 73rd cruise of the R/V *Akademik Mstislav Keldysh*, which took place in the Laptev Sea between September 21 and October 25, 2018, was to perform a set of biogeochemical, geophysical, and geological surveys in order to study methane venting (seeping) from bottom deposits, which were first detected in 2011 and evaluated quantitatively (Shakhova et al., 2015). The deployment of a local network of bottom seismographs was a component in this project. 20-year surveys carried out for the international ISSS project (International Siberian Shelf Studies) in East Arctic seas (EAS) showed that anomalies of dissolved methane and mass discharge of ebullition methane from bottom sediments into seawater and the atmosphere are due to degradation of undersea permafrost (Shakhova et al., 2009, 2010, 2014, 2017, 2019).

In the opinion of many scientists, seismotectonic events can affect the intensity of methane release and other components of geofluids (Field and Jennings, 1987; Kelley et al., 1994; Kusku et al., 2005; Bondur and Kuznetsova, 2012; Obzhurov, 2018; Sobisevich et al., 2018). In the case under consideration, the issue is about the influence of seismotectonic activity on fluxes of ebullition methane in the Laptev Sea shelf where over 80% of all undersea permafrost resides.

However, the first thing to do must be a study of bottom seismograph operation under the severe conditions of the Laptev Sea, of characteristic noise parameters, and the recording capability of the stations during different seasons. In addition, new data on the seismicity and present-day tectonics of the Laptev Sea region are urgently needed for engineering work on seismic hazard assessment to provide knowledge for running the Northern Sea Route and for development of hydrocarbon deposits in the Russian Arctic shelf.

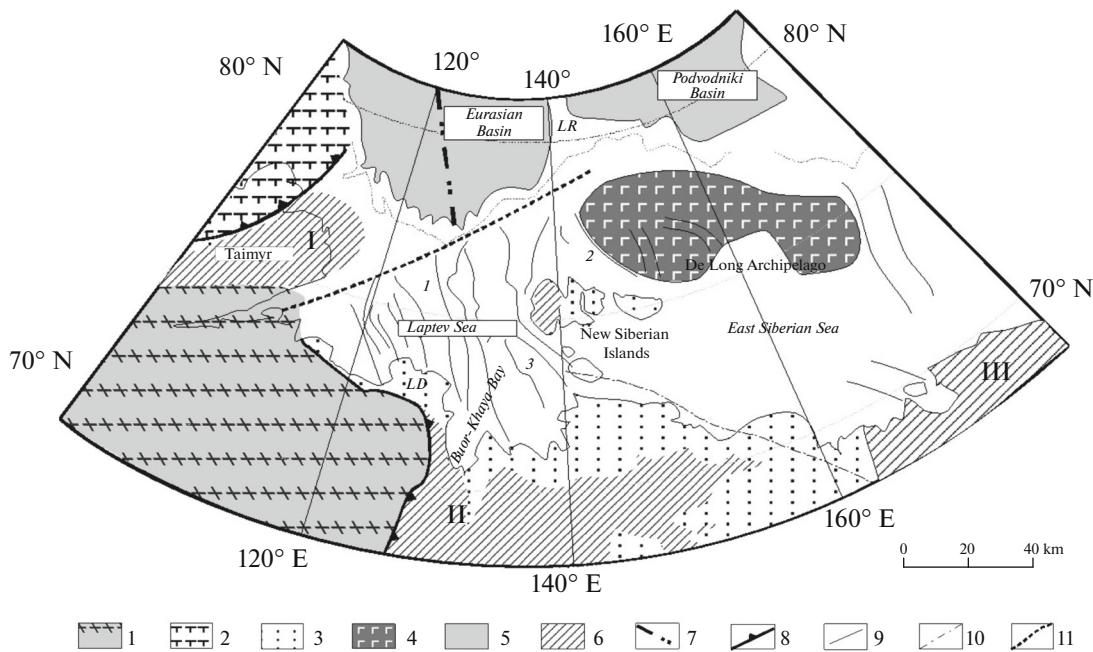


Fig. 1. A map of main structural features in the continental margin of the Laptev Sea and adjacent areas, after (Drachev, 2000a). (1) East Siberian craton; (2) Kara massif; (3) Cenozoic deposits; (4) De Long volcanic uplift; (5) oceanic deposits; (6) nappe-fold systems: Taimyr (I), Verkhoyansk–Kolyma (II), East Siberian–Chukchi (III); (7) Gakkel Ridge axial zone; (8) overthrust boundaries of fold belts; (9) normal faults (riffs: (1) Ust-Lena, (2) New Siberian, (3) Ust-Yana); (10) South Anyui suture zone; (11) Khatanga–Lomonosov fault; LR stands for Lomonosov Ridge and LD for Lena delta.

THE SEISMOTECTONICS OF THE LAPTEV SEA REGION

The Laptev Sea segment of the Arctic Ocean includes the water body above the Laptev Sea shelf and the adjacent onshore structures; it extends from the Taimyr Peninsula in the west to the New Siberian Islands in the east (Fig. 1). This is the area where meet structures of the Siberian Platform and of the Taimyr, Verkhoyansk–Kolyma, and Novosibirsk–Chukchi fold nappe systems. One characteristic feature peculiar to the Laptev Sea consists in a wide abundance of major rift structures that extend in the shelf away from the continental slope. The latter is adjacent to the southeastern flank of the Gakkel Ridge, which is part of the worldwide system of mid-oceanic ridges and which extends for over 1700 km (and is 80–160 km wide) from the North Atlantic (Bogdanov et al., 1998). The ridge shows rather high seismicity, while the seismicity in the rift zone that is an extension of the Gakkel Ridge onto the Laptev Sea shelf is diffuse (Avetisov, 2000, 2002). This zone is as wide as 500 km and about 700 km long, and consists of a sequence of sediment-filled grabens. The rift zones most likely overlie Late Paleozoic to Mesozoic fold belts (Drachev et al., 2010) whose structural material units are overlain by Upper Cretaceous and Cenozoic sediments 1.5 to 15 km thick. The Khatanga–Lomonosov shear zone serves as the boundary between the Gakkel Ridge and the Laptev Sea rift system (Drachev, 2000a, 2002).

The seismic belts in the Laptev Sea region are boundaries between the Eurasian and North American plates (Bogdanov et al., 1998; Avetisov, 2000). The westernmost boundary of the seismic region runs near the boundary of the thick lithosphere of the Siberian plate; the earthquakes do not occur, for the most part, deeper than 25 km beneath the continent and 10 km beneath the ocean (Franke et al., 2000; Fujita et al., 2009). It is hypothesized that the rotation pole is situated, most likely, south of the Lena River delta. Analysis of data on earthquake epicenters indicates that compression and tension phases give way to one another within very short distances. This may be due to the fact that the rotation pole is so near. Crustal tension, after (Franke et al., 2000), occurs in the eastern Laptev Sea region. The fault plane solutions are not reliable enough and show considerable scatter in the orientation of fault planes, so that the relevant tectonic displacements cannot be determined with sufficient detail.

The seismically active structures which are responsible for the formation of the Cenozoic marginal continental rift system mostly consist of northwest striking normal faults and strike slip faults that are nearly orthogonal to these. The normal faults bound a system of narrow grabens and depressions striking northwest, which is as long as 200–250 km and 40–60 km wide, and some submarine uplifts (Drachev, 2000a; Franke et al., 2001). The largest element of the rift system among these is the Ust-Lena Graben, which extends 400 to 420 km south from the southern tip of the Buor-

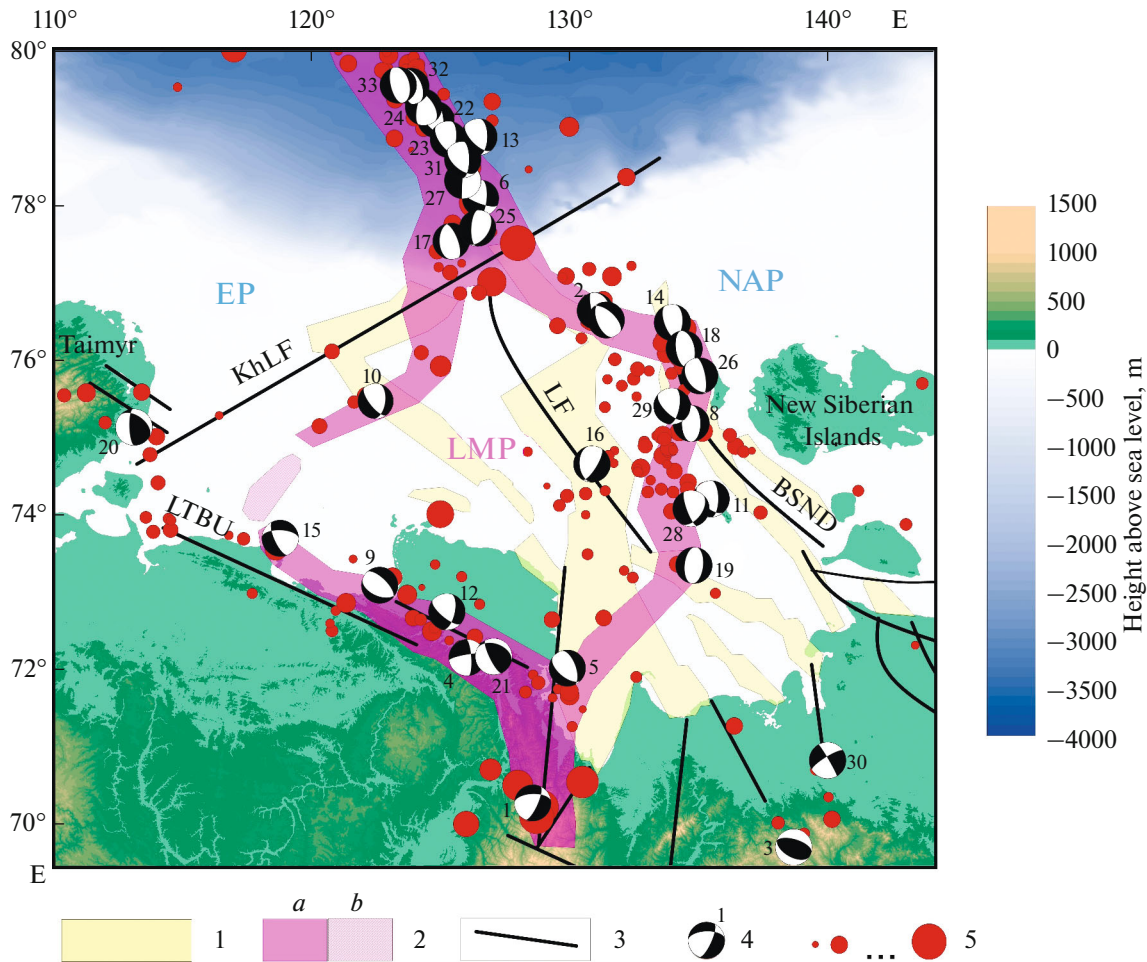


Fig. 2. A seismotectonic map of the Laptev Sea region, after (Avetisov, 2000; *Seismotektonika ...*, 2017) with modifications and additions.

(1) grabens on the Laptev Sea floor (*Seismotektonika ...*, 2017); (2) boundary of the Laptev microplate (Avetisov, 2000): *a* certain, *b* inferred; (3) main fault zones and individual faults; (4) epicenters and focal mechanisms of earthquakes (lower hemisphere) with their respective identification numbers (see Table 1); (5) epicenters of $3.0 < M \leq 6.8$ earthquakes, as reported by the ISC (*International ...*, 2020); EP Eurasian plate; NAP North American plate; LMP Laptev microplate; KhLF Khatanga–Lomonosov fault; LF Lazarev fault; BSND Belkovski–Svyatoi–Nos Depression; LTBU Lena–Taimyr zone of boundary uplifts.

Khaya Bay. The graben is as wide as 150–170 km in the north and gets gradually narrower to the south to shrink to 30–40 km. The graben structure is bounded by normal faults whose vertical amplitudes vary in the range 0.3–1.0 km throughout its length, and the graben is filled with sediments as thick occasionally as 10 km (*Seismotektonika ...*, 2017).

Another major lineament can be followed northwest from the Buor-Khaya Bay via the Lena R. delta into the Olenek and Anabar bays of the Laptev Sea, and further toward the Taimyr Peninsula. About 400 earthquakes have been recorded within it for the last 100 years; these earthquakes occurred at depths of 10–30 km and had energy class values $K = 7–14$ (magnitude $M \leq 6$) with several locations where the epicenter density is higher (*Seismotektonika ...*, 2017). This zone marks the Olenek Fault. The focal depths increase from 10

to 25 km southward in the direction of the Siberian continental margin. Exceptions are the focal mechanisms of the Taimyr earthquakes occurring in the western margin of the Laptev Sea shelf; their mechanisms indicate a compression setting (Imaev et al., 2000) (Fig. 2, Table 1).

It is of interest that the seismically active structures in the Laptev Sea were studied with a view to developing a long-term seismic model, several hundreds of thousands of years forward for numerical simulation of tsunami hazard on the coast (Kulikov et al., 2019a, b). A synthetic earthquake catalog was generated with the Monte Carlo method with subsequent numerical simulation of tsunami generation and propagation. The final step was to perform a statistical processing of calculated data in order to derive probabilistic estimates of tsunami runup heights that are likely to occur at the

Table 1. The source mechanisms of earthquakes in the Laptev Sea region for the observation period from 1927 to 2019

#	Date and origin time (h m)	φ° N	λ° E	h km	M_w	Source mechanism			Publication
						STK°	DIP°	$SLIP^\circ$	
1	14 Nov 1927 00:12	70.262	128.685	15	6.7	268	46	-35	F, 2009
2	3 Dec 1960 20:21	76.595	131.142	15	5.1	167	72	-90	F, 2009
3	19 Apr 1962 23:16	69.737	138.708	15	6.0	287	51	82	F, 2009
4	20 May 1963 17:01	72.162	126.517	15	5.5	356	70	-164	F, 2009
5	21 Jul 1964 09:56	71.989	129.934	13.9	5.5	130	45	-112	F, 2009
6	25 Aug 1964 13:47	78.035	126.557	15	6.7	111	64	-146	B, 1972
7	7 Apr 1969 20:26	76.481	131.227	15	5.5	157	45	-73	F, 2009
8	23 Apr 1977 14:49	75.191	134.494	10	4.9	180	45	-90	GCMT, 2020
9	1 Feb 1980 17:30	73.056	122.592	10.5	5.3	315	55	-78	GCMT, 2020
10	10 Jun 1983 02:13	75.427	122.495	15	5.6	142	59	-118	GCMT, 2020
11	12 Aug 1984 15:28	74.169	135.108	2.5	5.0	134	45	-126	F, 2009
12	15 Jun 1986 06:55	72.727	125.271	10	4.7	130	60	-134	F, 2009
13	22 Feb 1987 01:22	78.853	125.979	10	5.4	136	51	-122	GCMT, 2020
14	22 Sep 1987 22:05	76.403	134.375	11.6	5.5	159	52	-107	GCMT, 2020
15	25 Nov 1987 17:28	73.673	118.753	10	5.1	272	50	-142	F, 2009
16	1 Jan 1988 14:36	74.654	130.903	10	5.1	31	65	-73	GCMT, 2020
17	21 Mar 1988 23:31	77.523	125.476	15	6.4	339	58	-101	GCMT, 2020
18	5 Aug 1989 06:55	76.109	134.535	2.9	5.3	172	50	-87	GCMT, 2020
19	13 Mar 1990 00:32	73.325	134.898	15	5.3	186	45	-90	GCMT, 2020
20	9 Jun 1990 18:24	75.120	113.051	15	5.0	178	68	115	CK, 2017
21	1 Mar 1991 01:57	72.153	126.846	39.4	5.2	154	70	108	F, 2009
22	17 Feb 1992 00:02	79.161	124.679	15	5.9	355	54	-65	GCMT, 2020
23	21 Jan 1993 13:43	78.854	125.575	28.6	5.5	7	53	-59	GCMT, 2020
24	12 Feb 1993 10:52	79.212	124.507	19.7	5.0	193	59	-60	GCMT, 2020
25	5 Oct 1993 21:28	77.712	126.411	34.2	5.2	183	59	-106	GCMT, 2020
26	22 Jun 1996 16:47	75.812	134.962	15	5.8	349	63	-78	GCMT, 2020
27	19 Apr 1997 15:26	78.432	125.818	10	5.5	183	88	-88	USGS, 2020
28	7 Dec 2003 09:16	74.104	134.818	17.9	5.1	160	69	-118	GCMT, 2020
29	4 Jul 2008 04:55	75.398	134.039	19.3	5.0	10	54	-50	GCMT, 2020
30	29 May 2014 05:07	70.814	140.052	13.9	4.9	330	84	-162	GCMT, 2020
31	22 Jun 2014 23:58	78.526	125.832	10.6	4.8	360	59	-60	GCMT, 2020
32	27 Apr 2018 00:27	79.401	123.818	12	4.8	171	52	-80	GCMT, 2020
33	13 May 2019 00:43	79.408	123.897	19.5	5.3	166	54	-90	GCMT, 2020

The hypocenter coordinates (φ , λ , h) are from the GEM catalog, vol.7 (Storchak et al., 2013, 2015; Di Giacomo et al., 2018). Of the two possible fault planes at the source, we chose that which had the strike consistent with the main faults in the region. Publications: B, 1972 (Balakina et al., 1972); SK, 2017 (Seredkina and Kozmin, 2017); F, 2009 (Fujita et al., 2009); GCMT, 2020 (Dziewonski et al., 1981; Ekström et al., 2012; *Global ...*, 2020); USGS, 2020 (*U.S. Geological ...*, 2020).

coast. These calculations made it clear that the Laptev Sea coast is the most tsunami-prone among the coasts of the other arctic seas.

The subsidence of the shelf and coastal lowlands was a general phenomenon during Cenozoic time; it involved, not only individual grabens and depressions,

but also the intervening uplifts. The overthrusts and folds are overlain unconformably by Upper Pliocene horizontal deposits. This confirms the hypothesis that the extensional processes that were typical of the Cenozoic history of the shelf were disturbed by a compression episode at the end of the Miocene. Seismic

evidence shows that at present tension dominates the Laptev Sea shelf.

According to Imaev et al. (2000), faults of two directions have been active since the Cenozoic. The north–south faults typically show normal and reverse movements, while the east–west faults are dominated by differently directed shear displacements. It is emphasized that the axes of the paleotectonic movements are in satisfactory agreement with the directions of relative movement exhibited by the North American and Eurasian plates.

According to (*Seismotektonika ...*, 2017), sets of regional and local faults that were active during Cenozoic time can be identified in the southern continental circumference of the Laptev Sea. The kinematics of these zones is corroborated by cracking diagrams and by fault plane solutions for earthquakes. Four sets of fault zones can be identified on the basis of their spatial location, extent, and movements: the Coastal set of normal-oblique faults, the West Verkhoyansk overthrust system, the Kharaulakh normal-oblique fault system, and the Buor-Khaya normal fault system.

THE GEODYNAMIC MODELS OF THE REGION BASED ON LOCAL SEISMOLOGICAL OBSERVATIONS

The present-day tectonic processes that are occurring in the rift zone of the Arctic Ocean (the Gakkel Ridge) affect the shelf, which is seen as connectedness of shelf structures and the oceanic rift structures, as well as higher seismicity in the shelf area. The existence of the Laptev Sea rift system is explained by the fact that this region has been a segment of the boundary between the North American and Eurasian plates in the Arctic during the last 60–70 Ma (Drachev, 2000a).

Although there has been interest in the complex geodynamics of the region, until recently information on the seismicity in the Laptev Sea and its circumference was largely derived from records of teleseismic stations, thus furnishing a rather approximate idea of the epicenter distribution. The only thing that was clearly visible consisted in a well-pronounced linearity of the earthquake belt along the Gakkel Ridge and in an absence of the belt once we are in the shelf area; the seismicity was thus divided into an eastern and a western zone owing to the release of the stresses generated in the axial zone. As well, one hypothesized the existence of an axial seismic rift zone ascribed to the Ust-Lena depression; the zone passes through the middle of the shelf east of the Lena delta and reaches the continent via the Buor-Khaya Bay (Avetisov, 1993; Avetisov et al., 2001).

In addition to the several seismic stations operated by the Yakutia Branch of the RAS Geophysical Survey in the area of the village of Tiksi since the mid-1980s, we have few local instrumental seismological surveys in the Laptev Sea region (Fig. 3): the 1972–1976 expe-

ditions sent by the *PGO Sevmorgeologiya* (around the New Siberian Islands) (Avetisov, 1982) and some expeditions in 1985–1988 (the Lena R. delta and the shore of the Buor-Khaya Bay) (Avetisov, 1991). The result was to record numerous smaller events (magnitude below 4) in the Laptev Sea region and to make a seismological data bank for the Arctic region (Avetisov et al., 2001).

Separate mention must be made of the seismological experiment with ocean bottom seismometers in the Buor-Khaya Bay (Kovachev et al., 1994). Autonomous ocean bottom seismometers were used for seismic observations by researchers at the Institute of Oceanology (USSR Acad. Sci.) in the Buor-Khaya Bay in 1989 (see Fig. 3). Instruments with a surface buoy were installed in the bottom and held with a capron tether. A total of 68 microearthquakes have been recorded during three weeks, with 27 events being recorded by three or more stations. Hypocenters were determined for 26 microshocks with magnitudes $M_L = 0–2.5$. The results revealed a stable seismicity, to a first approximation, for the entire region and a local area within the region, because the slope of the recurrence curve for the microearthquakes was little different from that of the recurrence curve with $M > 4.5$ for the entire region of the mid-oceanic Gakkel Ridge. Remarkably enough, mantle seismicity has been identified at depths of below 65 km in the Buor-Khaya Bay area. As well, an unusual distribution of tectonic stresses over depth was identified in the Buor-Khaya crust, namely, the upper crust is dominated by compression, while the stresses at depths of 20–25 km are near zero (no seismicity occurs), and the lower crust and uppermost mantle is under tension. This circumstance suggested an original geodynamic model for the Laptev Sea shelf in which a bend in the lithosphere is hypothesized (Garagash et al., 1999; Kovachev et al., 2017).

An array of 17 bottom seismographs was deployed for one month in 2013 in the area of Muostakh Island in the southeastern Laptev Sea to determine the depth to permafrost using spectral ratios between horizontal and vertical components of seismic noise. The experiment made it possible to hypothesize that the permafrost top extends down to 20 m in sediments near the coastline. This is similar to the values obtained by electromagnetic surveying and borehole drilling at a depth of 4 m off Cape Buor-Khaya (Overduin et al., 2015). The method of electrical profiling was validated in a straightforward manner as part of a 5-year program of scientific drilling from on fast ice (2011–2015) in the Buor-Khaya Bay using 17 boreholes (as deep as 58 m) (Shakhova et al., 2017). The result was to demonstrate the absence of permafrost down to 100 m depth and deeper at most sites for sea depths over 4 m. The present study is the first phase of this work to detect relationships between seismotectonic activity and the spatial distribution of vents where ebullition methane is being discharged in the context of permafrost condi-

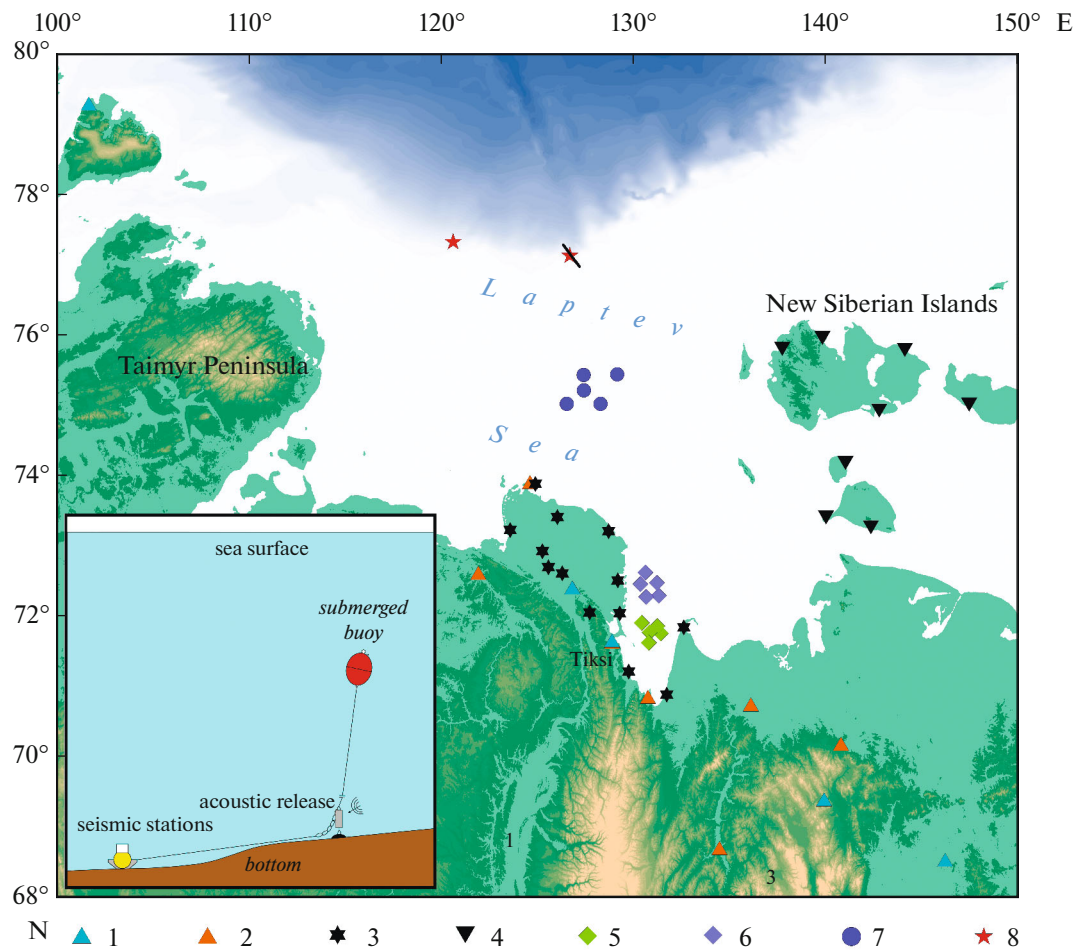


Fig. 3. The permanent and temporary networks of onshore and ocean bottom seismometers in the Laptev Sea region.

(1, 2) permanent and temporary seismic stations operated by the Geophysical Survey of the Russian Academy of Sciences (*Federalnyi ...*, 2020); (3, 4) temporary seismic stations during the 1985–1988 sequence of experiments (Avetisov, 1991) and during the 1972–1976 experiments (Avetisov, 1982), respectively; (5, 6) temporary ocean bottom seismometers during the 1989 experiments in the Buor-Khaya Bay (test sites 1 and 2, after (Kovachev et al., 1994, respectively)); (7, 8) temporary ocean bottom seismometers on the Laptev Sea shelf and in the continental slope during the first deployment in 2018–2019 (see Table 2), respectively; the crossed-out star marks the lost station; inset: ocean bottom seismometers deployment scheme in the shelf (sites 1–5) with a submerged buoy.

tion and elucidating the origin of methane sources (Shakhova et al., 2009, 2010, 2014, 2015, 2017, 2019).

The only obvious linear zone of interplate seismicity at the Gakkel Ridge branches out into two at the boundary with the continental margin, with its epicenters of larger earthquakes (magnitudes above 4) contouring the bulk of the Laptev Sea shelf. The epicenters of smaller events (magnitudes below 4) as recorded until present have a low density in the main water area of the shelf, and the relevant distribution is near diffuse. It is difficult to assign the seismicity to any fault system.

There are several geodynamic models for the peculiar modern tectonics of the Laptev Sea shelf. One of these (Avetisov, 2000, 2002) assumes a lithosphere microplate to exist in the Laptev Sea shelf, which is named the Laptev microplate (see Fig. 2). The model

is largely based on seismological observations, since the hypothetical Laptev microplate is bounded by the epicenters of comparatively large (magnitudes between 4 and 6) earthquakes.

Other researchers (Drachev, 2000b) hypothesize the existence of two microplates, the Ust-Lena and the East Laptev, with several possible options for configurations of their boundaries and for their kinematics. The model uses seismological data and the results of marine multi-channel seismic profiling (CDP reflection shooting), gravity data, and geological surveys of the continental circumference. There are also models (Lobkovsky, 2016) which describe microplates such as these as crustal features that can move laterally on the lower crustal plastic asthenolayer. Such models are based on an extension of the classical plate theory in which plates

are treated as deformable bodies, so that we have a tectonics of deformable plates. There is today no exhaustive proof in favor of any geodynamic model of the Laptev Sea region.

Overall, the available amount of recorded seismic events in the Laptev Sea region is obviously insufficient for an adequate description of its seismicity and geodynamic situation. The epicenters in the main shelf area as recorded today are sparse, and their distribution looks like that of scattered seismicity, so that it is difficult to assign them to any fault system. Consequently, there is lack of information from which to develop a detailed model of earthquake source zones. The scale and degree of detail in the existing generalized data base of linear and areal zones of possible earthquake generation for North Eurasia (Ulomov, 1999) as developed for the program of global seismic hazard assessment are insufficient for accurate assessment of seismic hazard in the Laptev Sea region. Hazard assessment is needed because of population centers existing in the region, as well as the infrastructure and its future development which are required to serve the operation of the Northern Sea Route and for developing hydrocarbon deposits in the shelf.

Because of this, a series of field surveys has been underway since 2016 conducted by a team from the Alfred Wegener Institute for Polar and Marine Research, Germany, from the Potsdam University, Germany, from the Shirshov Institute of Oceanology, Russian Academy of Sciences, and from the Yakutian Branch of the Geophysical Survey, Russian Academy of Sciences. This work aims at deploying temporary local seismic networks around the village of Tiksi and in the Lena R. delta according to the SIOLA project (Gaissler et al., 2018). At present records of two onshore experiments have been made, viz., 9-month records by a local network in the Lena R. delta (7–12 stations) and 13 stations southeast of Tiksi, which together make a small aperture seismic array (the 2016–2017 and 2017–2018 field seasons).

Thirteen $m_b \geq 4.3$ earthquakes have been recorded in the Russian area of responsibility in the Arctic region during the year 2017, of which 10 had epicenters north of Severnaya Zemlya, one east of Severnaya Zemlya, and two north of Franz Joseph Land. The largest earthquakes to have occurred in the Arctic region had a depth of 10 km north of Franz Joseph Land, both having $m_b = 5.7$ (Malovichko et al., 2018).

Eleven $m_b \geq 4.2$ earthquakes have been recorded in the Russian area of responsibility in the Arctic region during the year 2018; of these, 7 were north of Severnaya Zemlya, 1 east of Severnaya Zemlya, 2 north of Franz Joseph Land, and 1 north of Spitsbergen. Because the 2017 and 2018 epicenters were far from population centers, no felt data are available (Malovichko et al., 2019).

In addition, staffers of the Shirshov Institute of Oceanology of the RAS and Moscow Institute of

Physics and Technology deployed a temporary network of 7 broadband ocean bottom seismometers in the Laptev Sea shelf during 2018.

A NEW TEMPORARY NETWORK OF OCEAN BOTTOM SEISMOMETERS IN THE LAPTEV SEA SHELF. THE 73rd AND 78th CRUISES OF THE R/V *AKADEMIK MSTISLAV KELDYSH*

Seismotectonic events can affect the intensity of release for methane and other geofluid components, which may be seen in destabilization of hydrates, mass discharge of methane, the generation of funnels of varying diameter (from a few centimeters to a few hundred meters), in soil subsidence, and other georisks (Field and Jennings, 1987; Kelley et al., 1994; Kusku et al., 2005; Bondur and Kuznetsova, 2012; Obzhirov, 2018; Sobisevich et al., 2018). As well, methane can be endogenous, residing at depth; in that case it can come from great depths along faults and reach the level of gas hydrates where it can mix with near-surface methane. The presence of methane venting may be related to the existence of a rift system. Methane venting in the Laptev Sea may be related to the existence of a rift system. Major oil–gas deposits in sedimentary basins of the Arctic shelf are deep-seated sources of methane that migrates upward along rift faults. Small earthquakes that occur in zones such as these indicate active faults. For this reason local monitoring of microseismicity in the East Arctic seas can serve as an additional source of information on the origin of methane seeping, in addition to isotope techniques (Sapart et al., 2017).

The local network of ocean bottom seismometers was deployed on the Laptev Sea shelf during the 73rd cruise of the R/V *Akademik Mstislav Keldysh*, which took place between September 21 and October 25, 2018. The seismographs were retrieved during the 78th cruise of this vessel between September 16 and October 21, 2019.

The temporary local network which was recording on the Laptev Sea shelf in 2018–2019 consisted of five autonomous ocean bottom seismometers abbreviated as MBSSP (marine bottom station of seismoacoustic prospecting) (see Fig. 3). An MBSSP is equipped with a GG-7 hydrophone (manufactured by the IO RAS) with the frequency range 0.1–25000 Hz at 0.7 level, a unit of SME-4311 horizontal molecular–electronic broadband seismic sensors (manufactured by the OOO *R-sensors*) with the frequency range 0.016–50 Hz, a three-component unit of seismic sensors with a natural frequency of 10 Hz (two horizontal SG-10 and one vertical SV-10 sensor manufactured by the OOO *OIO-GEO Impulse International*) operating in the frequency band 10–200 Hz, an 8-channel seismic recorder that can GPS synchronize its inner clock, and a battery compartment. The sampling frequency is 100 Hz, hence the actual frequency range for all sensors is limited with an upper frequency of 40–50 Hz. The seismographs can operate in a self-contained

Table 2. The coordinates and dates of operation for ocean bottom seismometers on the shelf and continental slope of the Laptev Sea in 2018–2019 (for station locations consult Fig. 3)

Station no.	Latitude, deg. N.	Longitude, deg. E	Sea depth, m	Date of operation
1	75.01137	126.52483	37	6–9 Oct 2018
2	75.01173	128.26237	36	5–12 Oct 2018
3	75.20322	127.40412	40	6–8 Oct 2018
4	75.42210	127.39082	42	6 Oct 2018 to 8 Feb 2019
5	75.43138	129.13213	40	6 Oct 2018 to 8 Mar 2019
Slope 1	77.30772	120.60985	350	15 Oct 2018 to 31 May 2019
Slope 2	77.11362	126.68113	280	Lost

manner approximately 8 months with regard to power supply duration and memory capacity (32 GB), while the acoustic release can operate 1.5 years. As ice is present throughout most of the year in the Laptev Sea, these bottom stations were deployed with their buoys submerged (see Fig. 3, inset). The normal emergence of a submerged buoy is activated by an acoustic command transmitted to the acoustic release. The depth range of deployment, approximately 36–42 meters, can, on the one hand, prevent the stations to be damaged by pummock and, on the other, allows capturing a station by letting out the 120-meter rope between the station and the weight in case the acoustic release would fail.

In addition to the five-station array, two more pop-up ocean bottom seismometers were deployed on the shelf, on the continental slope at depths of 280–350 m. One of the two has been lost, while the records of the other require long preliminary technical processing and are so far not considered in this paper. In addition to the shelf stations, an ARV-K14-1 self-contained wave gauge (*OOO SKTB EIPA*, town of Uglich) has been deployed at site 3 (see Fig. 3). The recorder is designed for periodic recording of absolute pressure and temperature of seawater. The instrument is equipped with a pressure-sensitive quartz element whose membrane is bent under the action of a liquid column, deforming a force-sensitive piezo element attached to the membrane. The recording was carried out at a sampling frequency of 1 Hz (Table 2).

A study of seismic noise on records of ocean bottom seismometers revealed the fact that the noise situation on the bottom is critically dependent on the ice situation on the shelf. Figure 4 shows time-dependent spectrograms (sonograms) based on records of an SME-4311 broadband horizontal seismometer (a) and of a GG-7 hydrophone (b) deployed at site 5 (see Fig. 3), as well as records of the ARV-K14-1 self-contained wave meter (c) deployed at site 3 (see Fig. 3).

This choice of the station deployed at site 5 for noise analysis was due to the fact that its operation was the longest (of those stations that were deployed on the shelf), namely, 5 months, from October 6, 2018 to March 8, 2019. The wave gauge has been active all the

12 months. The time-dependent spectrograms based on records of the hydrophone and the seismometer were calculated using the window Fourier transform in a Hamming moving window of 2.5 hours for 50% overlap. The spectrograms based on records of the autonomous wave gauge were calculated using the Welch method (Welch, 1967) in a Kaiser–Bessel window of 48 hours for 50% overlap.

One can see in the spectrograms based on seismometer and hydrophone records that the signal is mainly amplified in the low frequency domain peaking at 01–0.2 Hz. The low frequency signal level dropped by three orders of magnitude (by ~60 dB) during November 1–2, 2018. A similar behavior was also exhibited by the spectrogram based on records of the self-contained wave meter. The highest amplification occurred at periods of 6–13 s, which is the range of wind waves and sea swell. The signal level of the autonomous wave gauge began to increase periodically since late April 2019, becoming invariably high in the later half of May, as was also the case in October.

Figure 5 shows fragments of ice maps developed at the AANII (*AANII* ..., 2020). Figure 5 is for the period October 28–30, 2018, when the Laptev Sea had extensive ice-free areas. During the next period, November 4–6, 2018 (Fig. 5b), the water was completely covered with young ice. It thus appears that the formation of continuous ice in the Laptev Sea occurred during the period between October 31 and November 4, 2018. It was during that period that seismic noise was much lower on records of the seismometer and the hydrophone, as well as on records of the wave gauge.

The time period when the Laptev Sea was completely covered with continuous ice lasted until April 21–23, 2019, which is demonstrated in Fig. 5c. The level of seismic noise and the wave gauge signal remained low. However, during the period to follow, April 28–30, 2019 (see Fig. 5d) there were areas with nilas, which is a thin elastic ice crust 0 to 10 cm thick that easily bends on water due to swell waves. Nilas areas had been present until May 19–21, 2019 (see Fig. 5e). The wave gauge signal began to recover gradually from mid-April until mid-May. Starting May 26–28, 2019

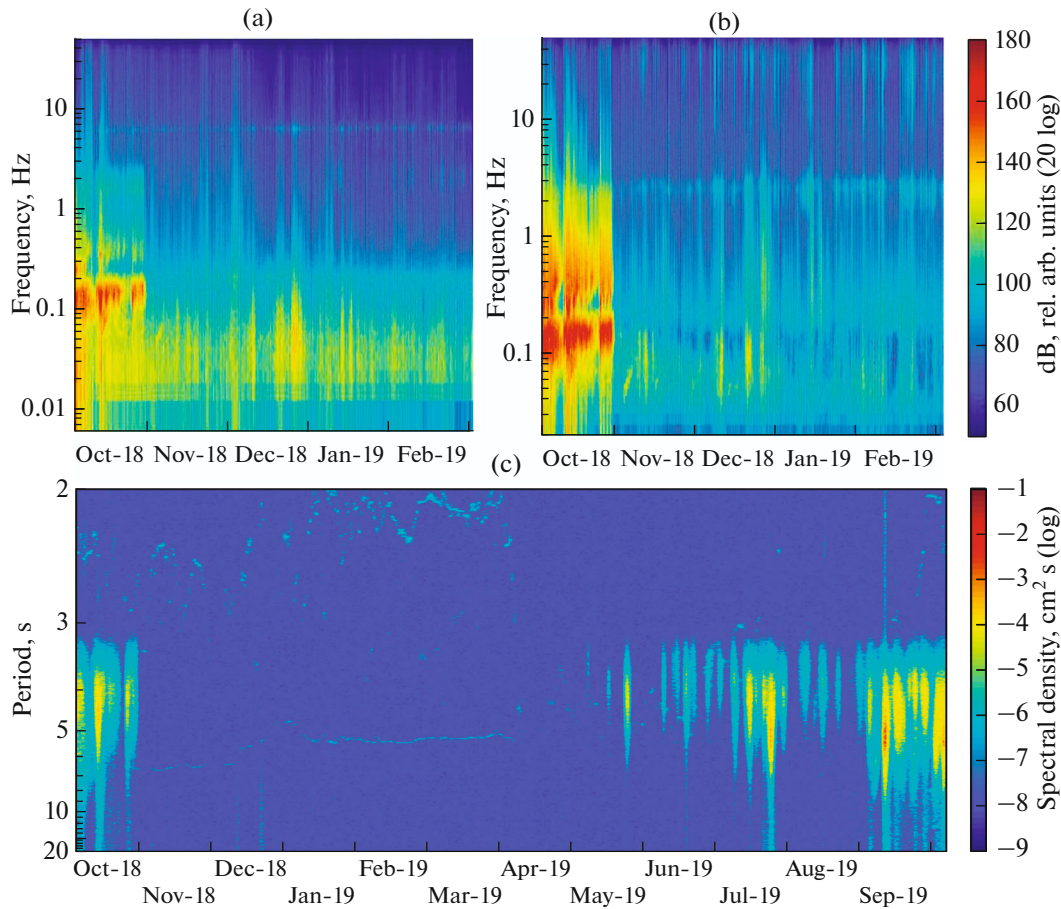


Fig. 4. Time-dependent spectrograms of noise (sonograms) based on records of an SME-4311 broadband horizontal seismometer (a) and of a GG-7 hydrophone deployed at site 5 (see Fig. 3) (b), as well as on records of the ARV-K14-1 autonomous wave gauge (c) deployed at site 3 (see Fig. 3).

(see Fig. 5f) when considerable areas of free water appeared, the wave gauge signal recovered the previous level, as in October 2018, at periods of 6–13 s. It can thus be concluded that the level of seismic noise in the Laptev Sea shelf at depths of 36–42 m strongly depends on the presence of wind waves and ice situation. The presence of continuous ice considerably reduces wind waves, hence diminishes the level of seismic noise.

Figure 6 shows curves of power spectral density (PSD) for seismic noise based on records of the same SME-4311 broadband horizontal seismometer at site 5. The PSD was found using the method of modified periodograms with preliminary determination of the autocorrelation series in a rectangular window of 5 h with subsequent averaging. The same figure shows curves for the NHNM (new high-noise model) and NLNM (new low-noise model) (Peterson, 1993), as well as extended NHNM and NLNM versions after (Wolin and McNamara, 2019), and the spectrum of SME-4311 self-noise. The relative positions of noise PSD curves based on seismograph records and the

curves for NHNM and NLNM can be used to infer the recording capabilities of the stations deployed.

The PSD curves for the time period of continuous ice in the Arctic region (shown in green) oscillate around the NHNM curve, and are similar in level to the spectra of island and coastal stations deployed in the Pacific at period $T \approx 0.1$ –10 s (Guan, Rarotonga, Rapanui, among others) (Peterson, 1993).

At the same time, one can see from Fig. 6 that the PSD curve for the time period of ice-free water lies above that for the period of continuous ice. The difference is by 20 dB in the short period domain, $T \approx 0.1$ s ($f \approx 10$ Hz); by 30 dB in the range $T = 1$ –5 s ($f = 0.2$ –1 Hz); and by 10 dB in the long period domain, $T > 13$ s ($f < 0.08$ Hz). The PSD curve during the ice-free period (blue) is everywhere above the NHNM curve, so that the identification of microearthquake signals on records requires special techniques.

At frequencies of 5–10 Hz, microseisms are generated by wave breaking (Webb, 1998). The PSD curves show a local maximum for both of the time periods at $T = 0.1$ –0.12 s ($f = 8$ –10 Hz) (see Fig. 6, marked 3).

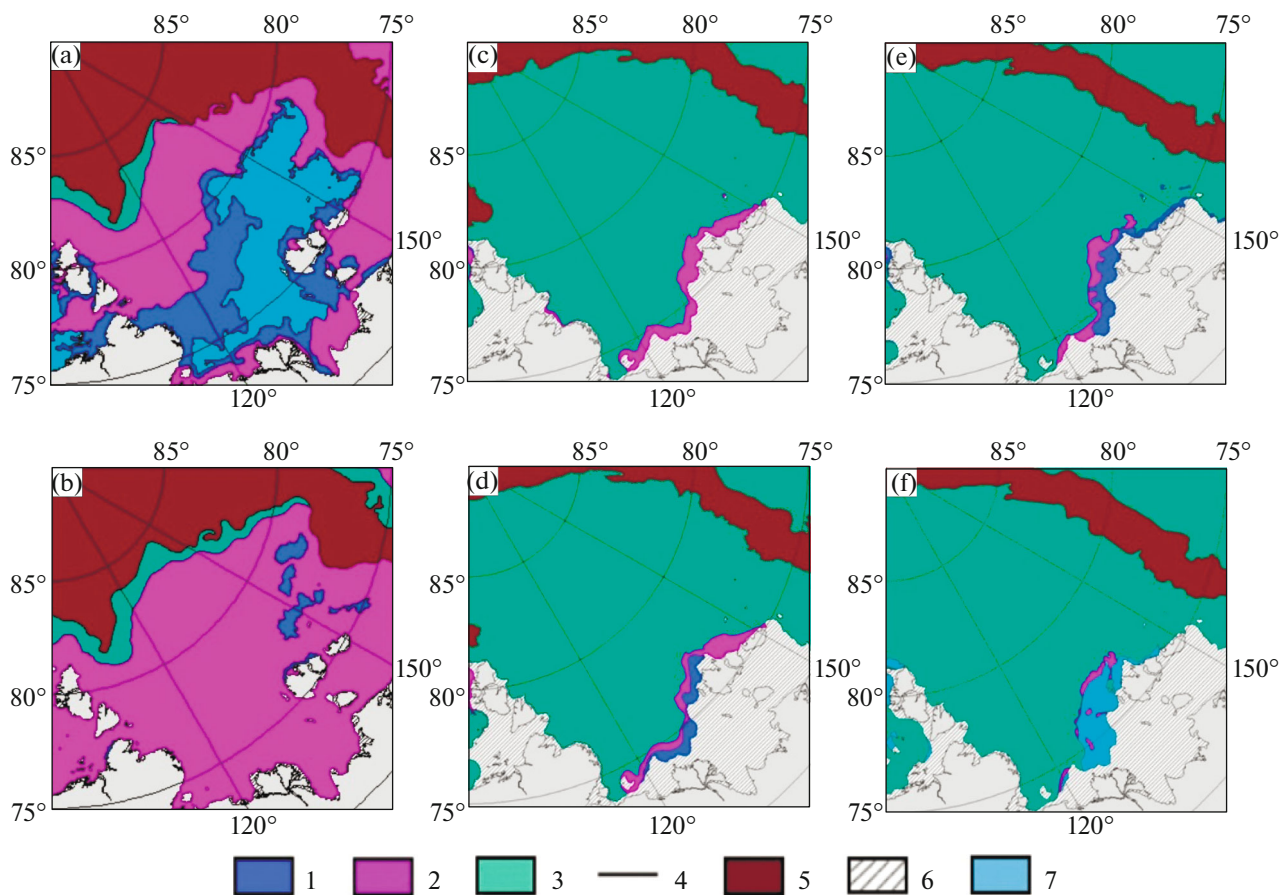


Fig. 5. The ice situation in the Laptev Sea as reported by the AANII of the Russian Hydrometeorological Agency (AANII ..., 2020) as of: (a) October 28–30, 2018; (b) November 4–6, 2018; (c) April 21–23, 2019; (d) April 28–30, 2019; (e) May 19–21, 2019; (f) May 26–28, 2019.

(1) nilas (1–10 cm); (2) young ice (10–30 cm); (3) one-year ice (30–200 cm); (4) boundaries of ice zones; (5) old ice; (6) fast ice; (7) clear water.

Maxima such as these on records of horizontal components at frequencies $f = 6–10$ Hz, in case the station was deployed on a soft soil, are explained by the so-called *coupling effect*, that is, by distortions at high frequencies due to parasitic oscillations in the station–weight–soft soil system (Webb, 1998).

One interesting fact consists in a persistent increasing noise level at long periods, no decrease occurring in the range $T = 4–11$ s, which is characteristic for the NHNM and NLNM curves. This type of PSD curve on seafloor has been reported in the literature, see, e.g., (Webb et al., 1998; Romanowicz et al., 1998; *New Manual ...*, 2012), and can be explained by tilting of bottom stations due to bottom currents. A sharp increase in PSD level at $T > 30$ s is also related to infragravitational sea waves (Webb, 1998).

The PSD curve for the time period corresponding to continuous ice is also characterized by a local maximum around the period $T = 6$ s (see Fig. 6, marked 1). The seismic noise components for spectral periods $T = 6 \pm 2$ s ($f = \sim 0.2$ Hz) carry the bulk of energy; they

are the so-called *secondary microseisms* (Webb, 1998; *New Manual ...*, 2012). According to the most popular hypotheses (Longuet-Higgins, 1950; Hasselmann, 1963), secondary microseisms are initiated by a standing wave that results from superposition of sea waves traveling in opposite directions. The original disturbances arise in areas of low air pressure above water (cyclones). From Fig. 6 it follows that the local maximum around $T = 6 \pm 2$ s is present during time periods with ice and that without ice (see Fig. 6, marked 1, 2). However, the spectral peak is much more pronounced during the ice-free period, in addition to a well-pronounced resonance whose main resonant period is $T_0 = 8 \pm 2$ s ($f_0 = 0.125$ Hz) and with extra resonant frequencies $3f_0, 5f_0, 7f_0$. This may tell us about the superposition of secondary microseisms and oscillations that are due to local fluctuations of hydrostatic pressure caused by wind waves.

The high level of seismic noise during the ice-free period leads to great difficulties for earthquake detection, at least during autumn (September and October)

when storms are frequent. The noise level is considerably lower (by as much as ~40 dB) during some individual short-lived calm windows. There were two calm windows, October 12–14 and 23–28 October, as can be inferred from the spectrograms in Fig. 4. It was during these periods that several signals from small local earthquakes were detected, while the rest of the October showed a very high noise that severely distorted the waveforms of transient signals. Several signals from small local earthquakes were detected on records between November 2018 and March 2019, when the sea was covered with continuous ice, as well as from moderate regional earthquakes, in addition to teleseismic signals due to distant earthquakes that were reported in international bulletins.

The coordinates and depths of recorded small earthquakes were not determined during the preliminary stage, mainly because no sensors for the vertical component of seismic signals were present in the bottom seismographs, because this component carries most information.

Figure 7 shows some sample waveforms and spectra of signals from a small local earthquake with magnitude $M_L = 2.0$ occurring at 17:12:54.65 UTC on November 28, 2018 at a distance of 30 km from the recording site (see Fig. 7a); from a regional $M_L = 3.5$ earthquake that occurred at 18:18:9.33 UTC on February 25, 2019 at a distance of about 500 km from the recording site (see Fig. 7b); and from a remote $M_s = 7.0$ event that occurred at a distance of 3400 km from the recording site (see Fig. 7c) (Alaska, November 30, 2018, 17:29:28.3 UTC).

The signal due to a small local earthquake shown in Fig. 7a has a wide frequency range, 1 to 40 Hz. The frequencies below 1 Hz have been filtered out, since they were stationary noise. The signal due to a regional earthquake (see Fig. 7b) has a narrow frequency range, 4 to 8 Hz. The frequencies below 2 Hz were contaminated with noise and have been filtered out to better visualize the earthquake waveform. The motion at frequencies above 8 Hz were lower because of attenuation. The signal due to the large teleseismic earthquake (see Fig. 7c) has a low frequency spectrum, 0.02 to 1 Hz, and includes a well-pronounced surface wave train.

The waveforms and spectra displayed in Fig. 7 suggest the inference that, during the period when seismic noise was lower owing to lower sea waves because of a complete calm or because the water was covered with continuous ice, the sensitivity and frequency responses of the GG-7 hydrophone and the SME-4311 seismometers used in the MBSSP are sufficient for reliable recording of both high frequency signals due to small local earthquakes and low frequency signals coming from large remote events.

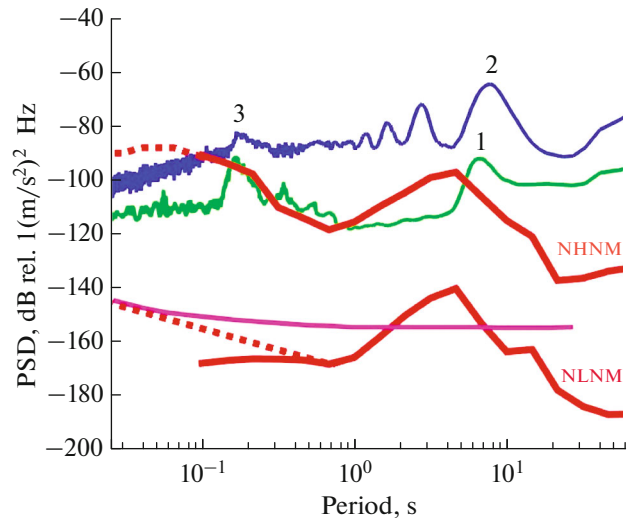


Fig. 6. The Power spectral density of seismic noise based on records of the SME-4311 broadband horizontal seismometer deployed at site 5 (see Fig. 3): blue line is for the period from October 6, 2018 to November 1, 2018 (clear water); green line is for the period from November 1, 2018 to March 8, 2019 (continuous ice). Solid red lines represent the NHNM (new high-noise model) and NLNM (new low-noise model) (Peterson, 1993); red dashed lines represent NHNM and NLNM after (Wolin and McNamara, 2020); violet line represents the curve of self-noise of the SME-4311 seismometer; numerals 1, 2, 3 mark local spectral extremums (see explanations in text).

Note: the expression of seismic noise PSD in dB involves the multiplier 10 to find the common logarithm.

DISCUSSION OF RESULTS

The experiment described above was the first attempt undertaken by the Institute of Oceanology to deploy ocean bottom seismometers on shelf in an Arctic sea during a whole year. No mention of similar surveys is available in the Russian periodicals. For this reason the issue of whether this experimental arrangement under ice conditions using these seismic stations and sensors can be utilized must be a subject of study.

The most important conclusion to be drawn from the experiment consists in the fact that the recording potential of a network of ocean bottom seismometers is strongly dependent on wind wave conditions. These are largely controlled by the degree of ice cover in the Laptev Sea, which can reduce the level of seismic noise by nearly three orders of magnitude (~30 dB for PSD). It seems that the recording capabilities of a network of ocean bottom seismometers are restricted to the winter periods of observation (November through April), as can be seen from observations of the ARV-K14-1 autonomous wave gauge (see the bottom panel in Fig. 4). As to the summer periods of observations, it is of interest to use the so-called “calm windows” in which the level of seismic noise is reduced to a minimum and it becomes possible to record small local earthquakes with acceptable resolution.

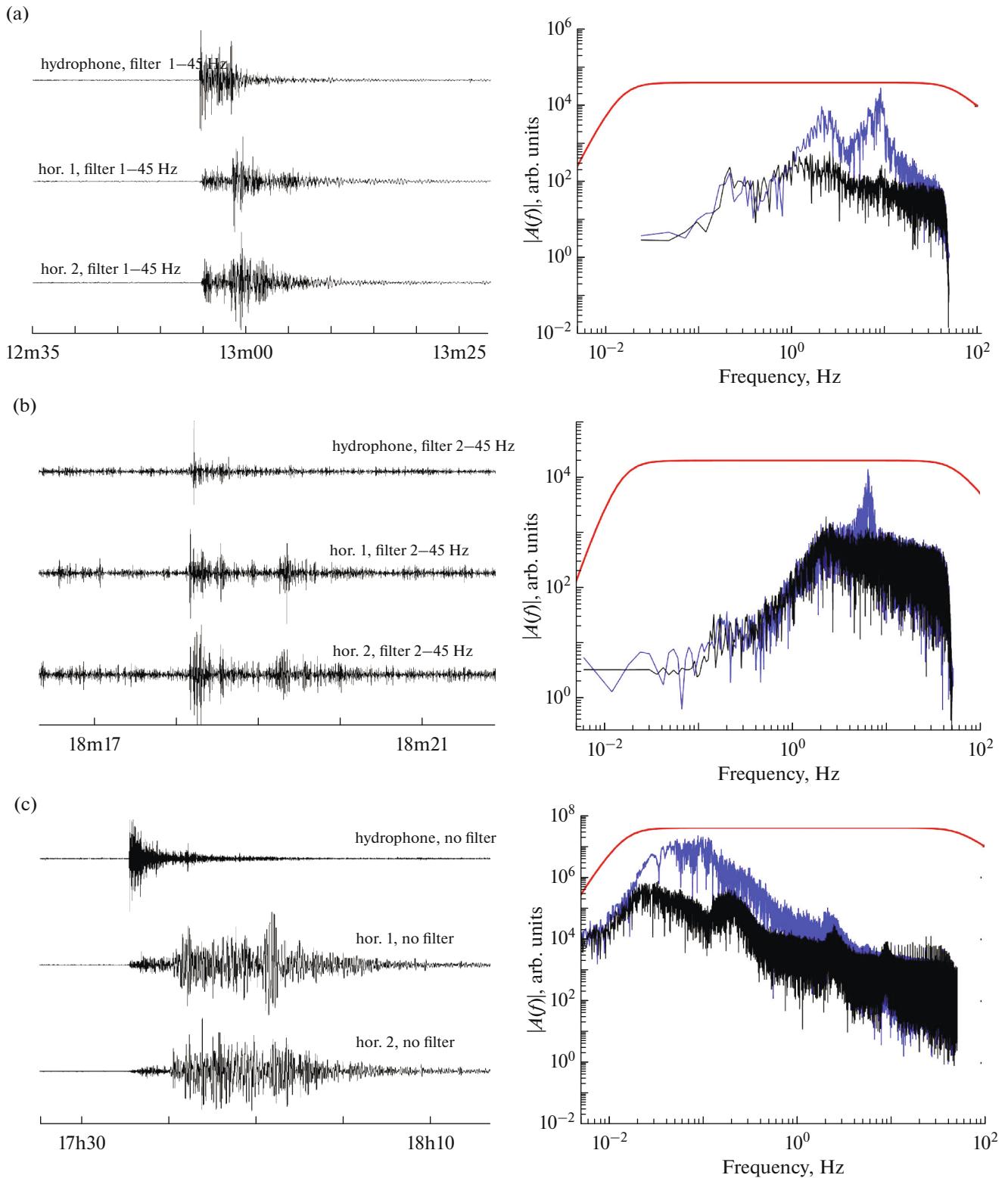


Fig. 7. Examples of recorded signals and their Fourier amplitude spectra due to a local microearthquake with magnitude $M_L = 2.0$ (November 28, 2018, 17:12:54.65 UTC) which occurred at a distance of 30 km from the recording site (a); a regional earthquake with magnitude $M_L = 3.5$ (February 25, 2019, 18:18:9.33 UTC) that occurred at a distance of about 500 km from the recording site (b); a remote earthquake with magnitude $M_S = 7.0$, (Alaska, November 30, 2018, 17:29:28.3 UTC) that occurred at a distance of 3400 km from the recording site (c). The red line represents the normalized response function of the SME-4311 seismometer, the blue line represents the Fourier amplitude spectrum of an earthquake signal (hor. 1 component, on filtering), and the black line shows the Fourier amplitude spectrum of noise (hor. 1 component, on filtering).

Another aspect of the experiment consists in the absence of records of bottom currents, making all reasoning as to the effect of currents on the noise characteristics of bottom seismographs rather speculative.

All the five MBSSPs were retrieved in 2019, a year after deployment. However, only one buoy floated up as envisaged after the acoustic release was activated. The other four stations were successfully retrieved by hooks dragging the 120-meter piece of rope laid on the bottom between a station and its weight. When the rope was caught by a hook, the buoys came up. It has turned out that all circuit breakers have been activated and dropped the weights, but the buoyancy of the buoys was insufficient to pull the rope from the bottom, probably from soil accretion. One of the pop-up stations deployed in the continental slope has been lost, because it could not be possible to establish connection to it via the hydroacoustic channel after one year of operation. The causes are not quite clear. Successful trawling of a pop-up station at a depth of about 300 m is extremely unlikely.

No station has been flooded, but only three stations yielded records lasting from four to seven months. The calculation of battery life at room temperature showed approximately eight months. The duration was probably reduced due to lower capacity of the alkaline batteries at a temperature about zero (on the bottom). Three more stations have operated during a few days only. This was caused by wires connecting the battery compartments being broken, probably because the stations were deployed during storms, entailing impacts on the ship hull and a hard landing on the bottom.

The lessons learned from the first year-long deployment of ocean bottom seismometers on the Laptev Sea shelf should be taken into account when planning future expeditions.

CONCLUSIONS

The present paper describes the current notions of seismotectonics and seismicity in application to the Laptev Sea region. Special emphasis is placed on a review of instrumental observations in the region, including the most recent ones conducted in the Laptev Sea shelf by deploying ocean bottom seismometers. New data on Arctic seismicity are urgently needed to detect a possible relationship between seismotectonic activity, the condition of undersea permafrost, and the release of methane of geological origin.

The most recent work to deploy temporary local networks of seismic stations started in the Lena River mouth in 2016 and in the Laptev Sea shelf in 2018 in order to fill the gap.

Comparative analysis of noise spectra based on records of a bottom seismograph, a hydrophone, and a wave gauge deployed in the middle of the Laptev Sea during the 73rd cruise of the R/V *Akademik Mstislav*

Keldysh showed that the noise amplitudes strongly depend on wind waves, which in turn depend on ice cover; hence the recording potential of a local network of ocean bottom seismometers is restricted to the winter period of observation.

ACKNOWLEDGMENTS

We are grateful to Corresponding Member of the RAS I.P. Semiletov who was the expedition leader of the 73rd and 78th cruises of the R/V *Akademik Mstislav Keldysh* (2018–2019), and to Academician L.I. Lobkovsky for managerial cooperation to conduct marine seismological operations during the cruises, to P.D. Kovalev for aid in organizing measurements of sea waves, as well as to the students of the MIPT and other members of the expedition for aid in shipboard operations to deploy and retrieve ocean bottom seismometers. As well, we thank B.V. Baranov, the head of the Laboratory of Hazardous Geological Processes, Institute of Oceanology RAS, for a comprehensive discussion of issues relevant to the tectonics of the Laptev Sea region.

FUNDING

This work was supported by State Assignment no. 0149-2019-0005 (a review of publications on seismicity and seismotectonics), by the State Program to Enhance Competitive Potential of Leading Universities in the Russian Federation among the Leading Science and Education Centers Worldwide (Program 5-100) (a description of local instrumental surveys), by the Russian Foundation for Basic Research, project no. 20-05-00533A (processing of ocean bottom seismometers records, analysis of seismic noise), no. 18-05-60250 (measurement and analysis of wind waves), and no. 18-05-01018 (analysis of earthquake catalogs). The field part of this study in the context of revealing characteristic features in the condition of undersea permafrost and the scale of ebullition methane release was carried out on board the R/V *Akademik Mstislav Keldysh* for the Russian Science Foundation (project no. 15-17-20032) and for the project of the Russian Government (no. 14, Z50.31.0012/03.19.2014).

REFERENCES

- AANII: Arctic and Antarctic Research Institute*, St. Petersburg, 2020. URL: <http://www.aari.ru/>
- Avetisov, G.P., The deep structure of the New Siberian Islands and adjacent water bodies as inferred from seismological data, *Sov. Geol.*, 1982, no. 11, pp. 113–122.
- Avetisov, G.P., Hypocenters and focal mechanisms of earthquakes in the Lena R. delta and its circumference, *Vulkanol. Seismol.*, 1991, no. 6, pp. 59–69.
- Avetisov, G.P., Some issues in the dynamics of the lithosphere beneath the Laptev Sea, *Fizika Zemli*, 1993, no. 5, pp. 28–38.
- Avetisov, G.P., Another remark concerning the earthquakes in the Laptev Sea, in *Geologo-geofizicheskie kharakteristiki litosfery Arkticheskogo regiona* (Geological and Geophysical Characteristics of the Lithosphere in the

- Arctic Region), St. Petersburg: VNIIOkeangeologiya, 2000, no. 3, pp. 104–114.
- Avetisov, G.P., On plate boundaries in the Laptev Sea shelf, *Dokl. Akad. Nauk*, 2002, vol. 385, no. 6, pp. 793–796.
- Balakina, L.M., Vvedenskaya, A.V., Golubeva, N.V., et al., *Pole uprugikh napryazhenii Zemli i mekhanizm ochagov zemletryasenii* (The Field of Elastic Stresses in the Earth and Earthquake Focal mechanism), Moscow: Nauka, 1972.
- Bogdanov, N.A., Khain, V.E., Rozen, O.M., et al., *Obyasnitelnaya zapiska k Tektonicheskoi karte morei Karskogo i Laptevykh* (An Explanatory Note to a Tectonic Map of the Kara and Laptev Seas), Moscow: Institut Litofery i vnutrennikh morei RAN, 1998.
- Bondur, V.G. and Kuznetsova, T.V., Identification of gas seeps in the Arctic seas using remote sensing data, *Issledov. Zemli Iz Kosmosa*, 2015, no. 4, pp. 30–43.
- Di Giacomo, D., Engdahl, E.R., and Storchak, D.A., The ISC-GEM Earthquake Catalogue (1904–2014): status after the Extension Project, *Earth System Science Data*, 2018, vol. 10(4), pp. 1877–1899.
- Drachev, S.S., The tectonics of the rift system on the bottom of the Laptev Sea, *Geotektonika*, 2000a, no. 6, pp. 43–58.
- Drachev, S.S., Laptev Sea rifted continental margin: Modern knowledge and unsolved questions, *Polarforschung*, 2000b, vol. 68, nos. 1–3, pp. 41–50.
- Drachev, S.S., On the tectonics of the basement beneath the Laptev Sea shelf, *Geotektonika*, 2002, no. 6, pp. 60–76.
- Drachev, S.S., Malyshev, N.A., and Nikishin, A.M., Tectonic history and petroleum geology of the Russian Arctic Shelves: an overview, in *Petroleum Geology: From Mature Basins to New Frontiers*, Vining, B.A. and Pickering, S.C., Eds., Proceedings of the 7th Petroleum Geology Conference, Published by the Geological Society, London, 2010, pp. 591–619.
- Dziewonski, A.M., Chou, T.-A., and Woodhouse, J.H., Determination of earthquake source parameters from waveform data for studies of global and regional seismicity, *Journal of Geophysical Research*, 1981, vol. 86(B4), pp. 2825–2852.
- Ekström, G., Nettles, M., and Dziewonski, A.M., The global CMT project 2004–2010: Centroid-moment tensors for 13,017 earthquakes, *Physics of the Earth and Planetary Interiors*, 2012, vols. 200–201, pp. 1–9.
- Federalnyi Issledovatel'skii Tsentr "Edinaya Geofizicheskaya Sluzhba Rossiiskoi Akademii Nauk" (Federal Research Center "Unified Geophysical Survey of the Russian Academy of Sciences", Obninsk, 2020. URL: <http://www.gsr.ru/new/struct/>
- Field, M.E. and Jennings, A.E., Seafloor gas seeps triggered by a northern California earthquake, *Marine Geology*, 1987, vol. 77(1–2), pp. 39–51.
- Franke, D., Hinz, K., Block, M., et al., Tectonics of the Laptev Sea Region in North-Eastern Siberia, *Polarforschung*, 2000, vol. 68, nos. 1–3, pp. 51–58.
- Franke, D., Hinz, K., and Oncken, O., The Laptev Sea Rift, *Marine and Petroleum Geology*, 2001, vol. 18(10), pp. 1083–1127.
- Fujita, K., Kozmin, B.M., Mackey, K.G., et al., Seismotectonics of the Chersky seismic belt, eastern Russia (Yakutia) and Magadan district, Russia, *Geology*, in *Geophysics and Tectonics of Northeastern Russia: A Tribute to Leonid Parfenov*, Stephan Mueller Special Publication Series, 2009, vol. 4, pp. 117–145.
- Gaessler, V.Kh., Baranov, B.V., Shibaev, S.V., et al., The Russian–German project "Seismicity and Neotectonics of the Laptev Sea Region", *Vestnik KRAUNTS, Nauki o Zemle*, 2018, no. 1, issue 37, pp. 102–106.
- Garagash, I.A., Kovachev, S.A., and Kuzin, I.P., Some results from the analysis of crustal stresses in the Buor-Khaya Bay, Laptev Sea, *Vulkanol. Seismol.*, 1999, no. 2, pp. 75–80.
- Global Centroid-Moment-Tensor (CMT) Project*, Electronic resource, 2020. URL: <http://www.globalcmt.org/>
- Hasselmann, K.A., A statistical analysis of the generation of microseisms, *Reviews of Geophysics*, 1963, vol. 1(2), pp. 177–209.
- Imaev, V.S., Imaeva, L.P., and Kozmin, B.M., *Seismotektonika Yakutii* (The Seismotectonics of Yakutia), Moscow: GEOS, 2000.
- International Seismological Centre*, Thatcham, Berkshire, United Kingdom. Electronic resource. 2020. URL: <http://www.isc.ac.uk/>
- Kelley, J.T., Dickson, S.M., Belknap, D.F., et al., Giant sea-bed pockmarks: Evidence for gas escape from Belfast Bay, Maine, *Geology*, 1994, vol. 22(1), pp. 59–62.
- Kovachev, S.A., Kuzin, I.P., and Soloviev, S.L., A short-term survey of microseismicity in the Buor-Khaya Bay, Laptev Sea using bottom seismographs, *Fizika Zemli*, 1994, nos. 7–8, pp. 65–76.
- Kovachev, S.A., Krylov, A.A., Ivanov, V.N., et al., The state of stress in the Laptev Sea microplate as inferred from marine seismological observations, *Estestvennye i Tekhnicheskie Nauki*, 2017, no. 4, pp. 52–57.
- Kulikov, E.A., Ivashchenko, A.I., Medvedev, I.P., et al., Tsunami hazard at the Arctic coast of Russia. Part 1. A catalog of probable tsunami-generating earthquakes, *Georisk*, 2019a, no. 2, pp. 18–32.
- Kulikov, E.A., Ivashchenko, A.I., Medvedev, I.P., et al., Tsunami hazard at the Arctic coast of Russia. Part 2. Numerical tsunami simulation, *Georisk*, 2019b, no. 3, pp. 6–17.
- Kuscu, I., Okamura, M., Matsuoka, H., et al., Seafloor gas seeps and sediment failures triggered by the August 17, 1999 earthquake in the Eastern part of the Gulf of Izmit, Sea of Marmara, NW Turkey, *Marine Geology*, 2005, vol. 215(3–4), pp. 193–214.
- Lobkovskii, L.I., The tectonics of deformable lithosphere plates and a regional geodynamic model in application to the Arctic and Northeast Asia, *Geol. Geofiz.*, 2016, vol. 57, no. 3, pp. 476–495.
- Longuet-Higgins, M.S., A theory for the generation of microseisms, *Philosophical Transactions of the Royal Society A, London*, 1950, vol. 243(857), pp. 1–35.
- Malovichko, A.A., Kolomiets, M.V., and Ruzaiкин, A.I., The seismicity of Russia in 2017, *Geoekologiya*, 2018, no. 6, pp. 59–68.
- Malovichko, A.A., Kolomiets, M.V., and Ruzaiкин, A.I., The seismicity of Russia in 2018, *Geoekologiya*, 2019, no. 4, pp. 51–60.
- New Manual of Seismological Observatory Practice (NMSOP-2)*, Bormann, P., Ed., Potsdam: Deutsches

- GeoForschungsZentrum GFZ, IASPEI, 2012. <https://doi.org/10.2312/GFZ.NMSOP-2>
- Obzhairov, A.I., On gas—geochemical precursors of seismicity increases, earthquakes, and volcanic occurrences in Kamchatka and in the Sea of Okhotsk, *Geosistemy Perokhodnykh Zon*, 2018, vol. 2, no. 1, pp. 57–68.
- Overduin, P.P., Haberland, C., Ryberg, T., et al., Submarine permafrost depth from ambient seismic noise, *Geophysical Research Letters*, 2015, vol. 42(18), pp. 7581–7588.
- Peterson, J., *Observation and Modeling of Seismic Background Noise*, U.S. Geological Survey Open-File Report, 1993, no. 93–322, pp. 1–95.
- Romanowicz, B., Stakes, D., Montagner, J.P., et al., MOISE: A pilot experiment towards long term sea-floor geophysical observatories, *Earth Planets and Space*, 1998, vol. 50(11–12), pp. 927–937.
- Spart, C.J., Shakhova, N., Semiletov, I., et al., The origin of methane in the East Siberian Arctic Shelf unraveled with triple isotope analysis, *Biogeosciences*, 2017, vol. 14, no. 9, pp. 2283–2292.
- Seismotektonika severo-vostochnogo sektora Rossiiskoi Arktiki* (The Seismicity of the Northeastern Sector of the Russian Arctic), Imaeva, L.P. and Kolodeznikov, I.I., Eds., (Institute of the Earth's Crust, Siberian Branch RAS, Institute of Geology of Diamonds and Noble Metals, Siberian Branch RAS), Novosibirsk: SO RAN, 2017.
- Seredkina, A.I. and Kozmin, B.M., The source parameters of the June 9, 1990 Taimyr earthquake, *Dokl. Akad. Nauk*, 2017, vol. 473, no. 2, pp. 214–217.
- Shakhova, N.E., Yusupov, V.A., Salyuk, A.N., et al., The human factor and emission of methane in the East Siberian shelf, *Dokl. Akad. Nauk*, 2009, vol. 429, no. 3, pp. 398–401.
- Shakhova, N., Semiletov, I., Salyuk, A., et al., Extensive methane venting to the atmosphere from sediments of the East Siberian Arctic Shelf, *Science*, 2010, vol. 327(5970), pp. 1246–1250.
- Shakhova, N., Semiletov, I., Leifer, I., et al., Ebullition and storm-induced methane release from the East Siberian Arctic Shelf, *Nature Geosciences*, 2014, vol. 7(1), pp. 64–70.
- Shakhova, N., Semiletov, I., Sergienko, V., et al., The East Siberian Arctic Shelf: towards further assessment of permafrost-related methane fluxes and role of sea ice, *Philosophical Transactions of the Royal Society A*, 2015, vol. 373, Article ID: 20140451.
- Shakhova, N., Semiletov, I., Gustafsson, O., et al., Current rates and mechanisms of subsea permafrost degradation in the East Siberian Arctic Shelf, *Nature Communications*, 2017, vol. 8, no. 15872.
- Shakhova, N., Semiletov, I., and Chuvilin, E., Understanding the permafrost–hydrate system and associated methane releases in the East Siberian Arctic Shelf, *Geosciences*, 2019, vol. 9(6), no. 251.
- Sobisevich, A.L., Presnov, D.A., Sobisevich, L.E., and Shurup, A.S., On the localization of discrete geological bodies as inferred from an analysis of the mode structure of seismoacoustic fields, *Dokl. Akad. Nauk*, 2018, vol. 479, no. 1, pp. 80–83.
- Storchak, D.A., Di Giacomo, D., Bondár, I., et al., Public release of the ISC-GEM global instrumental earthquake catalogue (1900–2009), *Seismological Research Letters*, 2013, vol. 84, no. 5, pp. 810–815.
- Storchak, D.A., Di Giacomo, D., Engdahl, E.R., et al., The ISC-GEM global instrumental earthquake catalogue (1900–2009): Introduction, *Physics of the Earth and Planetary Interiors*, 2015, vol. 239, pp. 48–63.
- U.S. Geological Survey. Electronic resource. 2020. URL: <https://earthquake.usgs.gov/earthquakes/search/>
- Webb, S.C., Broadband seismology and noise under the ocean, *Reviews of Geophysics*, 1998, vol. 36, no. 1, pp. 105–142.
- Welch, P.D., The use of Fast Fourier Transform for the estimation of power spectra: A method based on time averaging over short, modified periodograms, *IEEE Transactions on Audio and Electroacoustics*, 1967, vol. AU-15, no. 2, pp. 70–73.
- Wolin, E. and McNamara, D.E., Establishing high-frequency noise baselines to 100 Hz based on millions of power spectra from IRIS MUSTANG, *Bulletin of the Seismological Society of America*, 2020, vol. 110, no. 1, pp. 270–278.

Translated by A. Petrosyan